

Benchmarking of Force Fields for Molecule–Membrane Interactions

Markéta Paloncýová,[†] Gabin Fabre,^{†,‡} Russell H. DeVane,^{||} Patrick Trouillas,^{†,§,⊥} Karel Berka,^{*,†} and Michal Otyepka^{*,†}

[†]Regional Centre of Advanced Technologies and Materials, Department of Physical Chemistry, Faculty of Science, Palacký University Olomouc, tř. 17 Listopadu 12, 771 46 Olomouc, Czech Republic

[‡]LCSN EA1069, Faculté de Pharmacie, Université de Limoges, 2 Rue de Docteur Marcland, 87025 Limoges Cedex, France

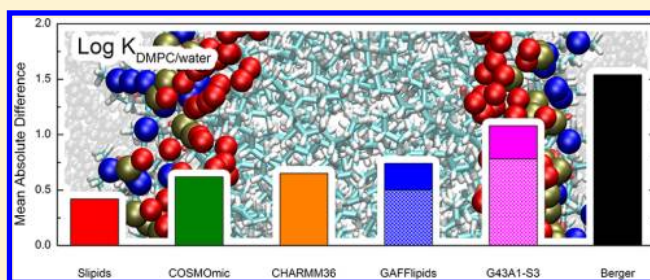
[§]INSERM UMR-S850, Faculté de Pharmacie, Université de Limoges, 2 Rue du Docteur Marcland, 87025 Limoges Cedex, France

^{||}Corporate Modeling and Simulation, Procter and Gamble, 8611 Beckett Road, West Chester, Ohio 45069, United States

[⊥]Laboratoire de Chimie des Matériaux Nouveaux, Université de Mons, Place du Parc 20, B-7000 Mons, Belgium

Supporting Information

ABSTRACT: Studies of drug–membrane interactions witness an ever-growing interest, as penetration, accumulation, and positioning of drugs play a crucial role in drug delivery and metabolism in human body. Molecular dynamics simulations complement nicely experimental measurements and provide us with new insight into drug–membrane interactions; however, the quality of the theoretical data dramatically depends on the quality of the force field used. We calculated the free energy profiles of 11 molecules through a model dimyristoylphosphatidylcholine (DMPC) membrane bilayer using five force fields, namely Berger, Slipids, CHARMM36, GAFFlipids, and GROMOS 43A1-S3. For the sake of comparison, we also employed the semicontinuous tool COSMOmic. High correlation was observed between theoretical and experimental partition coefficients ($\log K$). Partition coefficients calculated by all-atomic force fields (Slipids, CHARMM36, and GAFFlipids) and COSMOmic differed by less than 0.75 log units from the experiment and Slipids emerged as the best performing force field. This work provides the following recommendations (i) for a global, systematic and high throughput thermodynamic evaluations (e.g., $\log K$) of drugs COSMOmic is a tool of choice due to low computational costs; (ii) for studies of the hydrophilic molecules CHARMM36 should be considered; and (iii) for studies of more complex systems, taking into account all pros and cons, Slipids is the force field of choice.



INTRODUCTION

In nature, biomembranes make selectively permeable walls separating inner and outer cell environments, or inner organelles and cytosol.¹ They play a key role in the control of active transport and passive permeation of endogenous or exogenous compounds.^{2–4} Hence, the molecular interaction of xenobiotics (e.g., drugs and pollutants) with biomembranes is of major importance for understanding their flux through tissue and targeting in the human body.^{5–7} Biomembranes are complex supramolecular systems, which mostly consist of lipids arranged as bilayers. They also contain proteins attached or embedded in the membrane bilayer.⁸ The xenobiotics may interact with all these constituents during their passage through the membrane. Interactions of xenobiotics with the membrane-anchored cytochrome P450 represents a typical example of the complexity of membrane trafficking.^{9–11}

Basic features of the interaction of xenobiotics with biomembranes are known from experimental observations.¹² However, the understanding is fragmented and the molecular picture is often missing. Molecular dynamics (MD) simulations have appeared as an alternative way to gain insight into

structural features¹³ and thermodynamics of interaction of guest molecules with biomembranes.^{14–22} MD follows motions of all atoms of molecular system and generates a wealth of information having extremely fine resolutions both in time (subpicosecond) and space (atomic). This provides MD a major advantage with respect to all other techniques to tackle the interaction of xenobiotics with biomembranes, which nicely complements observations from the experimental techniques. On the other hand, the quality of MD simulations is heavily limited by the underlying empirical potential, also termed force field (FF), and affordable sampling, that is, duration of MD simulation.^{16,23,24} In other words, inaccurate FF parameters may lead to biased structural or thermodynamic membrane parameters, hence, developed FFs are tested to determine the level of agreement with experimental observations.

To date, numerous FFs have been developed for biomembranes, mostly focusing on structural and dynamical features of lipid bilayers. They were based on coarse-grained

Received: May 14, 2014

(e.g., MARTINI,²⁵ SDK²⁶), united-atom (e.g., Berger²⁷ and GROMOS 43A1-S3²⁸), and all-atom models (e.g., Slipids,^{29–31} CHARMM36,^{32,33} GAFFlipids,³⁴ LIPID11,³⁵ LIPID14³⁶). However, the accurate description of not only membrane structural parameters but also molecular interactions between guest molecules and biomembranes requires highly advanced FFs. For even more complicated goals such as membrane protein studies, they should also achieve a properly balanced description of structural and dynamical features of proteins. To this end, advanced FFs compatible with advanced protein FFs would be a promising tool to describe the behavior of guest molecules within realistic complex biomembranes.

To simulate thermodynamics of the interaction between a guest molecule and membrane with MD is computationally demanding as they require robust sampling and in turn accumulation of long simulation times.^{16,20} The huge computer cost of MD simulations has motivated many researchers to develop less expensive approaches to estimate thermodynamic properties of molecule–membrane interaction. An example of such approaches is the COSMOmic³⁷ tool of the COSMO-therm program,³⁸ which is based on the conductor-like screening model for realistic solvation (COSMO-RS) theory.³⁹ It was repeatedly shown that COSMOmic provides thermodynamics of molecule-membrane interactions in good agreement with experimental data.^{40,41} On the other hand, this implicit approach loses the fine time insight into the interaction, which is provided by MD simulations.

This study aims at a critical analysis of molecule-membrane interaction, as evaluated by free energy profiles, which were derived from z-constraint MD simulations. In the test set, 11 organic compounds were included, having a broad range of affinities for dimyristoylphosphatidylcholine (DMPC) bilayers and also bearing common organic functional groups. Five advanced FFs dedicated to biomembrane simulations have been evaluated, including Berger, Slipids, CHARMM36, GROMOS 43A1-S3, and GAFFlipids; for the sake of comparison, COSMOmic has been also employed. Based on free energies, the partition coefficients were calculated for each molecule and each FF and were compared to the available experimental data in order to investigate the performance of individual FFs for drug–membrane interactions.

METHODS

Small Molecule Parametrization. A set of 11 molecules was selected for which experimental partition coefficients to DMPC membrane were available (Table 1).⁴⁰ The molecules were chosen to cover a wide range of partition coefficients (from -1.04 to 5.64 measured at temperatures from 20 to 40 °C) and to include common functional groups present in drugs such as hydroxyl, carbonyl, chloro, methyl, nitro, and amino groups on aliphatic chains or aromatic benzene rings. The MD parameters of these molecules were prepared for individual FF, as recommended by their developers. Bonding and van der Waals parameters were taken from (i) GAFF⁴² for Slipids and GAFFlipids, (ii) PRODRG⁴³ for Berger and GROMOS 43A1-S3, and (iii) ParamChem^{44,45} for CHARMM36. For CHARMM36, partial charges were also taken from ParamChem. Special attention was paid to the description of partial charges for Slipids, GAFFlipids, Berger, and GROMOS 43A1-S3 FFs. For these FFs, the partial charges were derived using the restrained fit of electrostatic potential (RESP) procedure and the R.E.D. III software⁴⁶ using multiple conformations and multiple reorientations to ensure reproducibility of charge derivation, as ESP charges are sensitive to orientation.^{46,47}

Table 1. Molecules Used in This Study^a

no.	compd.	log K_{exp}	method	ref
1	glycerol	-1.04	Ultracentrifugation	52
2	methanol	-0.53	Ultracentrifugation	52
3	acetone	0.06	Ultracentrifugation (0.02 , 0.10)	52
4	1-butanol	0.51	Ultracentrifugation (0.54) Nondepletion PA-SPME (0.45)	52 53
5	benzylalcohol	1.14	Ultracentrifugation	52
6	aniline	1.63	Nondepletion PA-SPME	53
7	2-nitrotoluene	2.41	Nondepletion PA-SPME	53
8	<i>p</i> -xylene	2.98	Nondepletion PA-SPME	53
9	4-chloro-3-methylphenol	3.34	Nondepletion PA-SPME	53
10	2,4,5-trichloroaniline	4.16	Nondepletion PA-SPME	53
11	hexachlorobenzene	5.64	<i>n</i> -hexane passive dosing (5.43) PDMS sheet dosing (5.90) SPCE-PDMS passive sampling (5.59)	54 40 55

^aThe experimental partition coefficients (log K_{exp}) between water and DMPC are given from extensive data set.⁴⁰ They are given as an average of experimental values in case of multiple source of individual partition coefficients (shown in brackets in the Method column).

Conformations were generated from 1 ns MD simulation in vacuum followed by clustering using the single linkage method. Only clusters representing more than 10% of the total number of conformations were taken into account. Then, energy minimization and electrostatic potential (ESP) charges were calculated for each conformation with Gaussian09 (rev. A02)⁴⁸ either according to the Duan model⁴⁹ (B3LYP/cc-pVTZ and PCM solvation in diethyl ether) for Slipids, Berger, and GROMOS 43A1-S3 or according to the Cornell model⁵⁰ (HF/6-31G* in vacuum) for GAFFlipids.

MD Simulation Parameters. Fully hydrated membrane patches—bilayers were prepared with 36 DMPC lipids in each monolayer surrounded by 0.15 M NaCl solution to mimic the physiological conditions (Figure 1). The bilayers were then equilibrated and the simulation setup was tested against the experimental structural membrane properties.⁵⁶ The simulation setup was then used for the z-constraint simulation (see all specific simulation parameters for all FFs in Table 2). The bilayer normal was oriented parallel to the z-axis and the origin of the axis was set in the middle of the bilayer. All MD simulations were performed by the GROMACS 4.5.1 software package with a 2 fs time step and periodic boundary conditions in all directions. Electrostatic interactions were treated by the particle-Mesh Ewald method⁵⁷ and bonds were constrained by the LINCS algorithm.⁵⁸ A Parrinello–Rahman barostat⁵⁹ was used for a semi-isotropic pressure coupling at 1 bar and compressibility of 4.5×10^{-5} bar⁻¹ and Nosé–Hoover thermostat^{60,61} at 310 K.

Z-Constraint Simulation. Two drug molecules were initially placed in the simulation box: one in the middle of the membrane and another on the top of the simulation box, that is, into the water phase. The system was left for 500 ps to equilibrate and then both molecules were pulled in the same direction along the z-axis with a pulling rate of 0.05 nm·ns⁻¹ and a harmonic force constant of 500 kJ·mol⁻¹·nm⁻². The initial structures for z-constraint simulations were separated from this pulling simulation. In each simulation box two drug

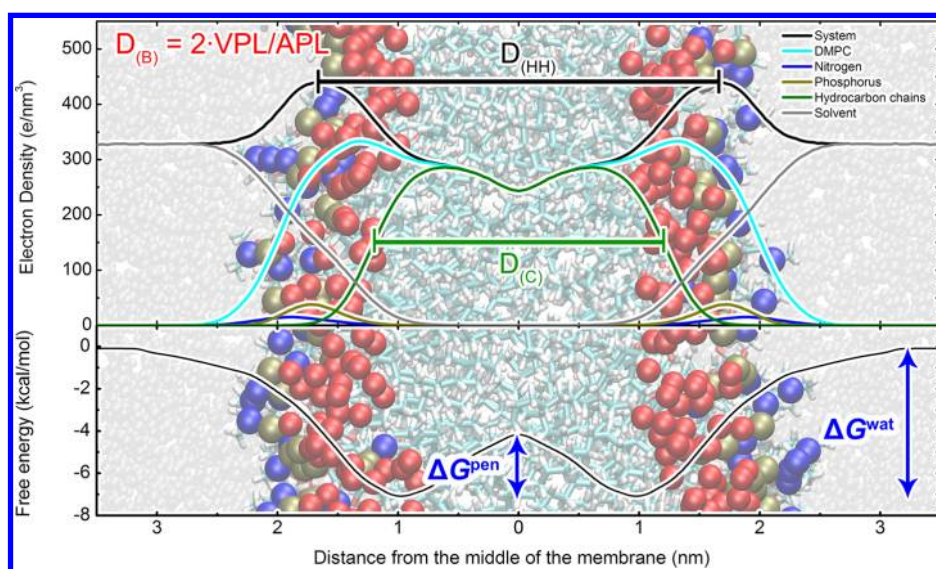


Figure 1. Structure of a dimyristoylphosphatidylcholine (DMPC) bilayer (background) with highlighted glycerol oxygens (red balls), choline nitrogens (blue) and phosphorus (dark yellow). The electron density profile (upper panel) contains labels for membrane thicknesses, that is, headgroup to headgroup distance ($D_{(HH)}$), hydrocarbon core thickness ($D_{(C)}$), and Luzzati thickness ($D_{(B)}$) calculated as a ratio of volume per lipid (VPL) and area per lipid (APL). The free energy profile (lower panel) has highlighted water/lipids barrier ΔG^{wat} , representing the affinity to the membrane, and penetration barrier ΔG^{pen} .

Table 2. Simulation Parameters^a

force field	R_{coulomb} (nm)	R_{vdw} (nm)	$R_{\text{vdw-switch}}$ (nm)	bond constraints	water model	RESP method/basis set	CPUh/project
Berger	1.0	1.0		all-bonds	SPC/E ^{62,63}	B3LYP/cc-pVTZ	21 200
GROMOS 43A1-S3	1.0	1.6		all-bonds	SPC/E ^{62,63}	B3LYP/cc-pVTZ	34 400
CHARMM36	1.4 (1.2)	1.4 (1.2)	0.8	H-bonds	CHARMM TIP3P ⁶⁴		145 200
Slipids	1.0 (1.0)	1.5 (0.9)	1.4 (0.8)	all-bonds	TIP3P ⁶⁵	B3LYP/cc-pVTZ	71 300
GAFFlipids	0.8	0.8		H-bonds	TIP3P ⁶⁵	HF/6-31G*	44 900
COSMOmic							3

^a R_{coulomb} is a short-range electrostatic cut-off, long-range electrostatics are evaluated by PME, R_{vdw} is Lennard-Jones cut-off, in case of switching off the Lennard-Jones interactions, the switching begins at $R_{\text{vdw-switch}}$. In case of CHARMM36 and Slipids, we tested the structural parameters also using different cut-off lengths (in brackets, not affecting the total CPU time in this table). CPUh/project display the total CPU hours for the calculations—for obtaining the topologies and 30 ns z-constraint simulations for MD simulations and for DFT calculations and final free energy profile calculation in case of COSMOmic. The detailed CPU times are in Supporting Information Table S2.

Table 3. Mean Differences (MDi) and Mean Absolute Differences (MAD) of Water/Lipids ΔG^{wat} and Penetration ΔG^{pen} Barriers with Respect to Data Obtained from Slipids FF^a

force field	ΔG^{wat}		ΔG^{pen}	
	MDi (kcal/mol)	MAD (kcal/mol)	MDi (kcal/mol)	MAD (kcal/mol)
Berger	1.94	2.09	0.14	1.06
CHARMM36	−0.27	0.72	−0.15	0.89
GAFFlipids	0.02 (0.14)	0.72 (0.68)	1.04 (0.33)	1.33 (0.65)
GROMOS 43A1-S3	−0.34 (−1.07)	1.65 (1.12)	−0.35 (−0.29)	1.28 (1.31)
COSMOmic	0.12	0.91	−0.73	0.91

^aThe values in brackets show the differences with excluded outlier (2-nitrotoluene in GROMOS 43A1-S3 and acetone in GAFFlipids).

molecules were placed, one in each monolayer. The windows for z-constraint simulations were chosen with separating distance of 0.3 nm, whenever possible.

Z-constraint simulations constrain a distance between different groups and monitors the required force applied on the molecule to keep this distance. The averaged force is then used to calculate the free energy profile also called potential of mean force (eq 1):

$$\Delta G(z) = - \int_{\text{outside}}^{z'} \langle \vec{F}(z) \rangle_t dz \quad (1)$$

where $\langle F(z) \rangle_t$ is the force applied on the molecule in order to keep it at a given depth z . We constrained the two molecules in a box and monitored the applied force separately. Over the last years, we have systematically optimized the simulation protocol for free energy profile calculation in order to minimize the computer time cost.¹⁷ Several authors have identified that the selection of an initial structure can slow the convergence of free energy profiles, especially in area of head groups.^{16,20,66} The z-constraint simulation converges quicker compared to umbrella simulation, even when the initial structure is unequilibrated.¹⁶ As it was also successfully used earlier,⁶⁶ the

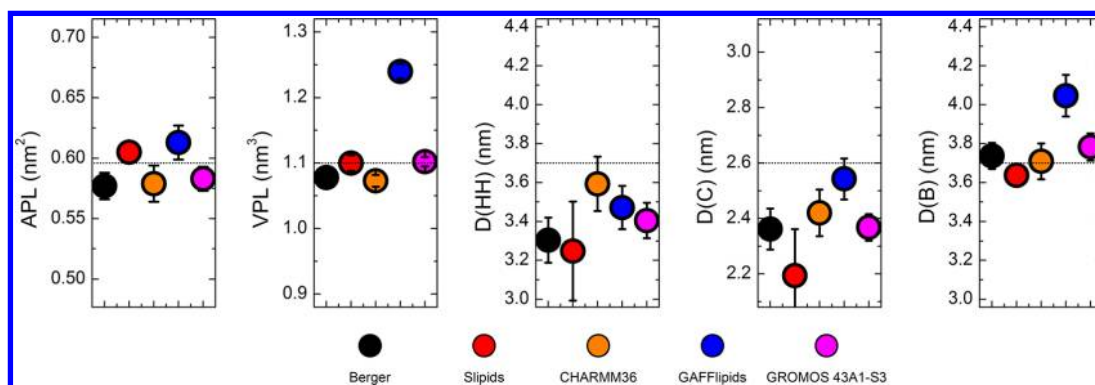


Figure 2. Structural parameters of DMPC bilayer as predicted by MD simulations with various FFs compared to experimental values at 30 °C shown as dotted lines.⁵⁶ APL, area per lipid; VPL, volume per lipid; $D(\text{HH})$, electron–electron density peak distance; $D(\text{C})$, hydrocarbon core thickness; $D(\text{B})$, Luzzati thickness. The error bars show the standard deviation of data obtained from multiple simulations, all the graphs are scaled to show 20% of deviation from experimental values.

amount of simulation windows was halved by adding two solute molecules in one simulation box. Free energy profile by z -constraint simulation allows a window of 0.3 nm. This significantly reduces the computing-time cost. It should be noted that cutoff lengths and water models dramatically influence computational time (Table 3). The z -constraint simulations were run for 30 ns per simulation window and the convergence of free energy profiles was monitored. The initial 15 ns of constraint simulation were left for equilibration and the free energy profiles were calculated from the last 15 ns. In the case of too slow convergence, the window lengths were extended to 50 ns (see the Supporting Information Table S1).

COSMOmic Free Energy Profile Calculation. To increase the precision of COSMOmic calculations, 30 DMPC bilayer structures obtained from Slipids simulation were used; this approach was successfully applied in earlier works.^{17,41} The geometries and σ -profiles of DMPC, water, and guest molecules were obtained by DFT/COSMO calculations at the BP/TZVP level of theory.^{67,68} A single conformation as a result of geometry optimization was used. Free energy profiles were calculated at 310 K. Using the COSMOmic software³⁷ from the COSMOtherm 13 package, the bilayers were separated into 50 layers.⁶⁹ A total of 162 orientations of the solute molecules were used for each membrane to produce individual free energy profiles. The final free energy profile was averaged over the individual free energy profiles of all the DMPC bilayer structures.

Log K Calculation. The free energy profiles obtained with MD (all FFs) and COSMOmic were analyzed and the partition coefficients were calculated according to an implemented method of COSMOmic^{37,41} that removes the need for setting a membrane border and which is independent of the system size (eq 2):

$$K = \int_0^n \left(e^{-\Delta G(z)/RT} - \frac{\rho_{(z)}^{\text{water}}}{\rho_{(n)}^{\text{water}}} \right) dz \frac{\text{APL}}{M_{\text{lipids}} m_u} \quad (2)$$

where $\Delta G(z)$ stands for a free energy at depth z , $\rho_{(z)}^{\text{water}}$ stands for water density at depth z , and $\rho_{(n)}^{\text{water}}$ stands for density of bulk water. The multiplying factor converts the partition coefficient into units used in experimental works $\text{kg}(\text{lipid})/\text{L}(\text{water})$. APL is the area per lipid, M_{lipids} is the molecular weight of lipids and m_u is the atomic mass constant.

Statistical Evaluation. Predicted $\log K_{\text{calc}}$ were compared to the $\log K_{\text{exp}}$ experimental values in terms of mean difference

(MDi) $(1/N \sum_i^N (\log K_{\text{calc},i} - \log K_{\text{exp},i}))$ and mean absolute difference (MAD) $(1/N \sum_i^N |\log K_{\text{calc},i} - \log K_{\text{exp},i}|)$, and in terms of the parameters of the linear $\log K_{\text{exp}}$ vs $\log K_{\text{calc}}$ fit (eq 3):

$$\log K_{\text{exp}} = a \cdot \log K_{\text{calc}} + b \quad (3)$$

which was constructed by the least-squares method. The significance of the slope differing from 1 and intercept differing from 0 were evaluated at the probability level of 0.975. We analyzed the outliers of $\log K$ predictions based on a Williams plot⁷⁰ and identified acetone in GAFFlipids, 2-nitrotoluene in GROMOS 43A1-S3, and 2-nitrotoluene and hexachlorobenzene in Berger. Due to the limited number of molecules investigated, we included the outliers in our analysis. However, for analysis in a given FF, the outliers were excluded. We also analyzed the predictability of proper ordering of molecules according to their lipophilicity based on Spearman's rank correlation coefficient. Further we analyzed the heights of free energy barriers—the water/lipids barrier ΔG^{wat} , the membrane center penetration barrier ΔG^{pen} and the free energy at various membrane depths—and compared them to the values from Slipids that provided $\log K_{\text{calc}}$ in the best agreement with experimental data.

RESULTS AND DISCUSSION

Structure of DMPC Bilayer Is Well Represented by All FFs. During both unbiased and z -constraint simulations, most of the membrane structural parameters stayed reasonably close to experimental values,⁵⁶ though most of the FFs produced a bilayer with thickness lower than that measured experimentally (Figure 2). The values of area per lipid (APL) were reproduced reasonably well by all FFs considered here. The volume per lipid (VPL) predicted by GAFFlipids significantly differed from the other FFs. On the other hand, GAFFlipids showed headgroup distance ($D(\text{HH})$) and hydrocarbon thickness ($D(\text{C})$) in agreement with the experimental data. The Luzzati thickness ($D(\text{B})$), which depends on a ratio of VPL and APL (see Figure 1 for thickness explanation),⁵⁶ was again well reproduced by all other FFs but GAFFlipids (Figure 2). In summary, all FFs tested in this study accurately reproduce the structural features of the DMPC bilayer reasonably well.

Additional relevant structural characteristics of fluid membranes are the order parameters of lipid tails.⁷¹ The average order parameters were monitored (i.e., both sn1 and sn2 chains

were averaged, Figure 3) during both unbiased and z-constraint simulations. Slipids, Berger, and GROMOS 43A1-S3 FFs

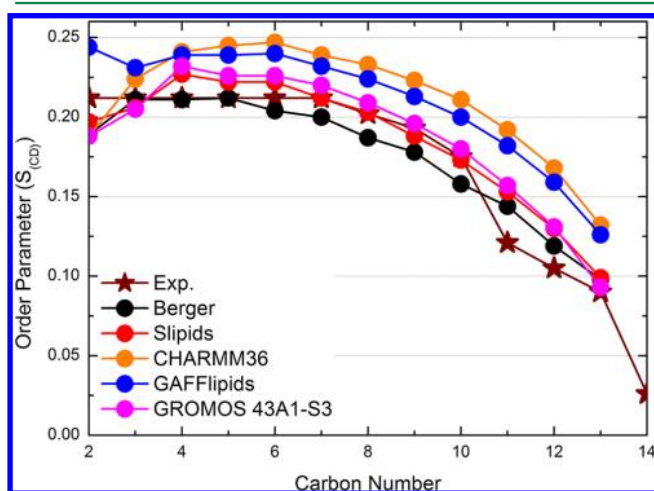


Figure 3. Order parameters experimentally measured (stars) and calculated by MD simulations with five FFs.

reproduced the order parameters as best (MAD equal to 0.012, 0.013, and 0.015, respectively). On the other hand, the order parameters calculated by GAFFlipids and CHARMM36 were slightly overestimated (MAD 0.031 and 0.035). These findings agree with a recent work by Piggot et al.,¹³ comparing structural parameters of DPPC and POPC; the calculated order parameters of lipid tails in the plateau region below the head groups were the lowest with Berger, followed by GROMOS 43A1-S3 and CHARMM36. It should be noted that in the original publication of GAFFlipids³⁴ the order parameters were also slightly overestimated. However, DMPC membranes were in fluid phase with all FFs, for the full simulation time.

The structural features of the DMPC membrane are sensitive to the simulation setup, especially cut-offs and water models. So, we used the setup suggested by the developers of each FF and when necessary we optimized the setup to acquire structural parameters best agreeing with the experimental data (see Table 2). As expected, from the point of view of computational time, the united atom FFs (i.e., Berger and GROMOS 43A1-S3) were the most efficient (Table 1 and Supporting Information Table S2). There were also differences among the all-atom FFs, the most effective being GAFFlipids due to a very short cutoff (0.8 nm). Slipids take advantage of uncharged carbons and hydrogens in the middle of aliphatic tails, while CHARMM36 was the slowest among all tested FFs, because of the long cutoff used, and the CHARMM modified TIP3P water model. In order to use parameters compatible with AMBER ff99SB FF for proteins, we also carried out Slipids simulations with 1.0 nm cutoff and tested CHARMM36 simulations with a 1.2 nm cutoff. In this case, the DMPC bilayer structural parameters stayed reasonably close to the experimental values (data not shown). Decreasing the cutoff is an attractive way to increase performance for future simulations on larger membrane systems.

Calculated Partition Coefficients Agreed with the Experimental Values. Membrane/water partition coefficients were calculated by eq 2 and compared with the experimental values (Table 1 and Supporting Information Table S2). The relative ranking of the molecules according to their partition coefficients, which was evaluated by the Spearman's rank order correlation coefficient, was reproduced best by Slipids and CHARMM36 (Supporting Information Table S2). The differences in ranking appeared for the medium lipophilic molecules for both CHARMM36 and Slipids, while both FFs ranked all lipophilic molecules properly. CHARMM36 ranked adequately even the most hydrophilic molecules ($\log K < 0.5$) while Slipids ranked well all molecules with $\log K$ higher than 1.7. The COSMOmic approach also ranked properly the lipophilic

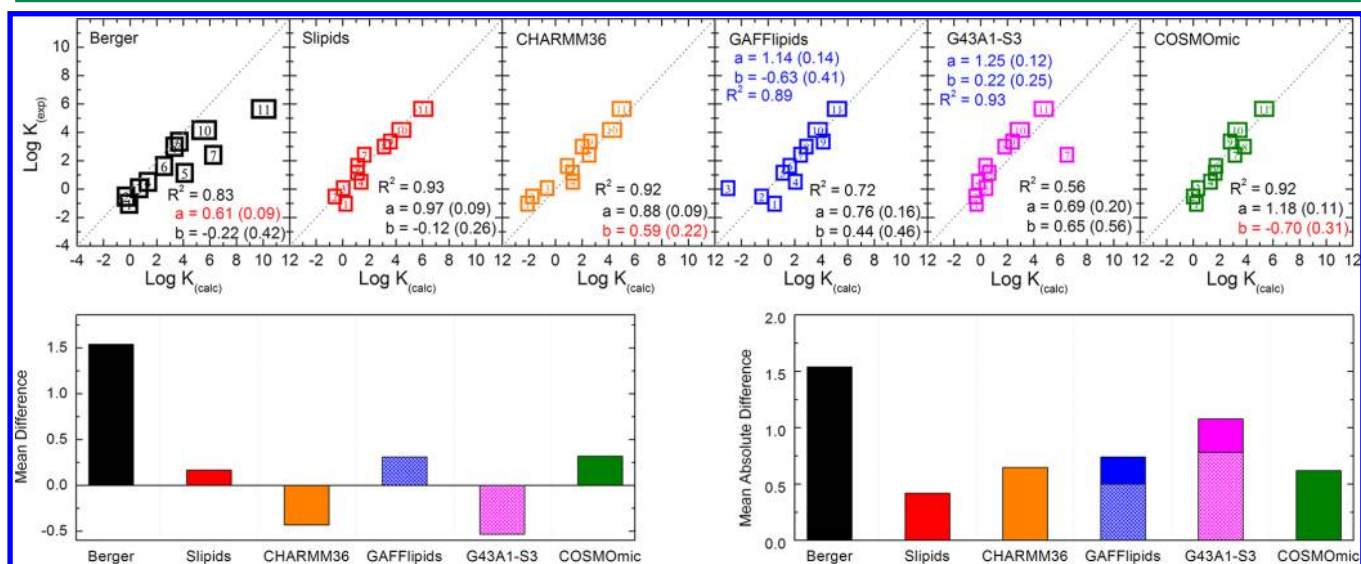


Figure 4. Experimental partition coefficients plotted against the respective calculated values (upper panel) with parameters of the linear fit, that is, coefficient of determination, R^2 , slope (a) (standard deviation in bracket) and intercept (b). Slopes significantly differing from 1.0 and intercepts from 0.0 significantly on the probability level of 0.975 are highlighted in red. Each data point is labeled by a number, which corresponds to the number of the molecule in Table 1. The fitting parameters for GROMOS 43A1-S3 (G43A1-S3) and GAFFlipids recalculated by omitting outliers (acetone and 2-nitrotoluene, in GAFFlipids and GROMOS 43A1-S3, respectively) are shown in blue. The bar charts (lower panel) depict the mean differences and the mean absolute differences (MAD). The patterned bars show values when excluding outliers.

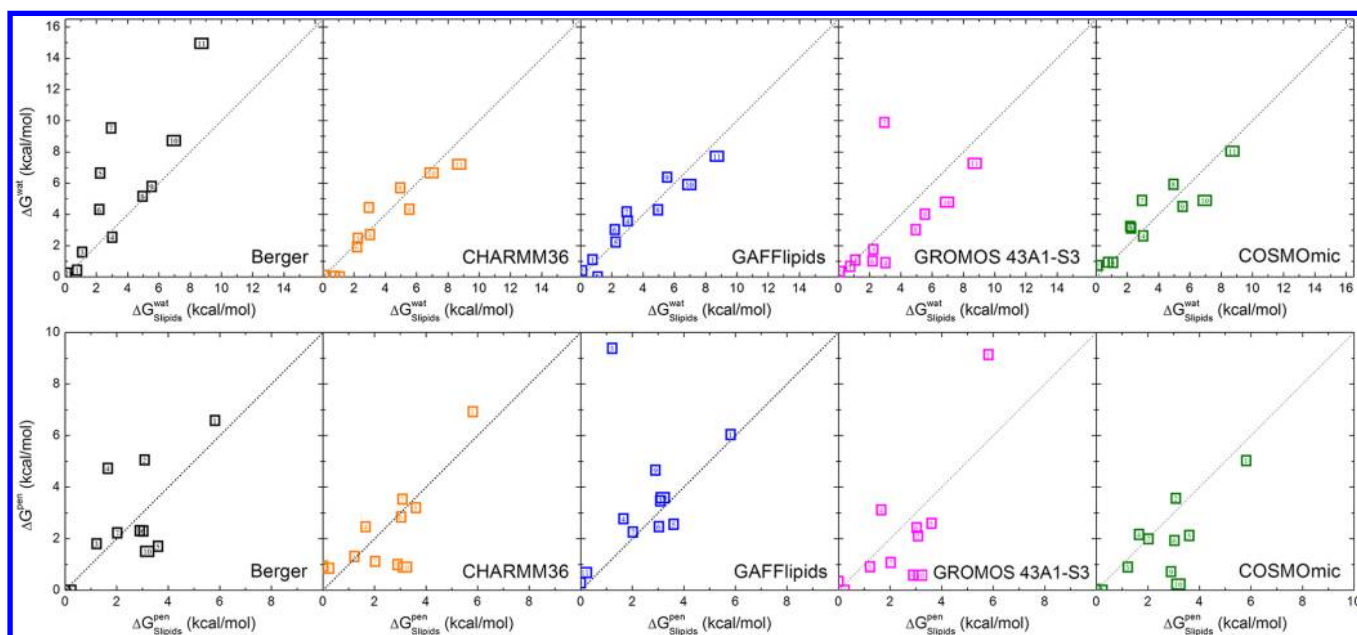


Figure 5. Water/lipid barriers ΔG^{wat} and penetration barriers ΔG^{pen} calculated by all FFs and COSMOmic vs the values obtained with Slipids.

molecules and performed just a little worse than Slipids and CHARMM36. GAFFlipids, Berger, and GROMOS 43A1-S3 showed worse ranking performance over the whole lipophilicity scale (Supporting Information Table S2). It should be stressed that all FFs and COSMOmic reproduce the right ranking of affinities to DMPC membrane, with $\alpha = 0.05$ statistical significance.

The absolute predicted values of the partition coefficients $\log K_{\text{calc}}$ also agreed with the corresponding experimental values $\log K_{\text{exp}}$ (Figure 4, Supporting Information Table S3). The mean absolute difference with respect to $\log K_{\text{exp}}$ of $\log K_{\text{calc}}$ obtained with Slipids was 0.42 log unit, which is comparable with the experimental uncertainty for determination of $\log K_{\text{exp}}$. With this FF, the linear fit between calculated and experimental partition coefficients (cf. eq 3) led to a slope of effectively 1 and a y -intercept of effectively 0 (0.97(0.09) and $-0.12(0.26)$, respectively, see Figure 4). CHARMM36 and COSMOmic exhibited similar performance (MAD 0.65 and 0.62, respectively), but CHARMM36 showed systematic shifts toward hydrophilic results ($b = 0.59(0.22)$), whereas COSMOmic toward hydrophobic results ($b = -0.70(0.31)$). GAFFlipids (MAD 0.74) gave one outlier (acetone), and GROMOS 43A1-S3 (MAD 1.08) gave 2-nitrotoluene as outlier. When omitting the outliers the mean absolute differences dropped to more reasonable values, namely 0.50 and 0.78 for GAFFlipids and GROMOS 43A1-S3 FFs, respectively. The reason for the existence of these respective outliers has not been rationalized. Berger FF is known to overestimate lipophilicity of guest molecules and showed the largest deviation from experimental values.¹⁷ In summary, taking the mean absolute differences and the linear fit of $\log K$ into consideration, the best performing FF among those tested here appears to be Slipids. However, the other FFs appear predictive enough, with the significant exception of Berger FF. Taking the predictive power (see also ref 17) into consideration and regarding low computer cost, COSMOmic can be recommended for high throughput screening of interaction of small molecules, for example, drugs, cosmetics, antioxidants, pollutants, pesticides, and warfare agents with lipid bilayers.

Properties of the Free Energy Profiles. From the previous section, Slipids was taken as a reference, and the performance of the other FFs was tested in terms of water/lipids barrier ΔG^{wat} and penetration barrier ΔG^{pen} with respect to the corresponding values obtained with Slipids. The water/lipid barriers ΔG^{wat} (that strongly correlates with $\log K_{\text{calc}}$, $r^2 = 0.96$) predicted by CHARMM36, GAFFlipids, and COSMOmic were similar to those obtained with Slipids (Table 3, Supporting Information Tables S4, S5, and Figure 5). GAFFlipids exhibited the lowest mean difference (MDI 0.02 kcal/mol) and both GAFFlipids and CHARMM36 yielded the best mean absolute difference (MAD 0.72 kcal/mol, or even better—0.68 kcal/mol—when excluding the acetone outlier from GAFFlipids data set). ΔG^{wat} values calculated by GROMOS 43A1-S3 exhibited a MAD 1.65 kcal/mol; when removing the 2-nitrotoluene outlier from the data set, the MAD dropped to 1.12 kcal/mol. Berger as expected predicted higher values of ΔG^{wat} with a MAD of 2.09 kcal/mol due to its over attractive Lennard-Jones interactions as we suggested earlier.¹⁷

Concerning the mean difference of the penetration barrier ΔG^{pen} , the best agreement with Slipids was achieved with CHARMM36 having a MDI -0.15 kcal/mol and a MAD 0.89 kcal/mol. COSMOmic predicted ΔG^{pen} values lower than Slipids with a MDI -0.73 kcal/mol and a MAD 0.91 kcal/mol. The mean absolute difference calculated from GAFFlipids data was 1.33 kcal/mol (and 0.65 if acetone was excluded). The mean absolute differences calculated from GROMOS 43A1-S3 and Berger data were 1.28 and 1.06 kcal/mol, respectively. Though ΔG^{pen} range is lower the range of ΔG^{wat} with Slipids (5.8 and 8.7 kcal/mol, respectively), the relative mean absolute difference (with respect to Slipids) of ΔG^{wat} of CHARMM36, COSMOmic, and GAFFlipids is less than or equal to the mean absolute difference of ΔG^{pen} . Therefore, CHARMM36, COSMOmic, and GAFFlipids agreed with Slipids better for ΔG^{wat} than ΔG^{pen} . However, it must be stressed that in the case of GAFFlipids, the ΔG^{pen} description was affected by the presence of one outlier (Figure 5). On the other hand, the mean absolute difference of both free energy barriers of CHARMM36 and COSMOmic compared to Slipids was lower

than 1.0 kcal/mol. This confirms the ability of Slipids, CHARMM36, and COSMOmic to provide comparable and rather accurate predictions of the free energy barriers.

The free energy profiles were also compared at different membrane depths calculated by all methods vs the free energy profile from Slipids (Figure 6). The reference free energy value

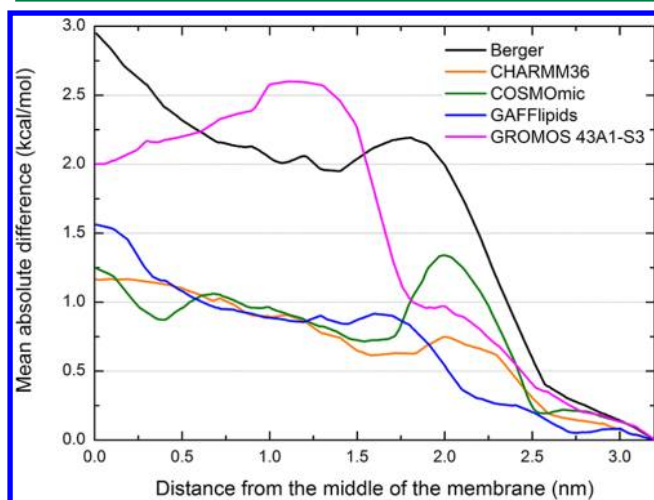


Figure 6. Mean absolute difference of free energy profile values with respect to Slipids as a function of distance from the middle of the membrane.

($\Delta G = 0$ kcal/mol) was set to water and the largest increase in the differences occurred at the water/membrane interface (2.5–1.5 nm from the membrane center). For COSMOmic, the maximum mean absolute difference (MAD 1.3 kcal/mol) was reached at 2.0 nm, dropped back to 0.7 kcal/mol at 1.75 nm, and slowly increased again to 1.2 kcal/mol in the middle of the membrane. With CHARMM36, it increased gradually up to 1.2 kcal/mol at the membrane center and the bump at the interface is less pronounced. GAFFlipids exhibited a slightly similar behavior with a mean absolute difference below 1.0 kcal/mol except at the center of the membrane. Berger and GROMOS 43A1-S3 failed in the description of the free energy profiles with respect to Slipids. Berger produced an excessively lipophilic description (i.e., too deep, Supporting Information Figure S1) with a mean absolute difference reaching 2.9 kcal/mol in the center of the membrane. Concerning the united atom FFs, GROMOS 43A1-S3 is a better choice than Berger and all-atomic FFs and COSMOmic performed better than any of the united atoms FFs.

CONCLUSION

This work compared the performance of five (two united atom and three all atom) FFs and the implicit COSMOmic method to reproduce the experimentally observed partition coefficients of 11 molecules into the DMPC membrane. Slipids appeared to be the most precise method, followed by COSMOmic, CHARMM36, GAFFlipids, GROMOS 43A1-S3, and Berger. COSMOmic and the all-atomic FFs performed well and reproduced the log K with a mean absolute difference lower than 0.8 log units. Perhaps a more relevant result is that Slipids, CHARMM36, and COSMOmic performed well in the prediction of free energy barriers; GAFFlipids predicted ΔG^{wat} very well. In terms of computational time, COSMOmic is by far the best choice at predicting log K for fluid membranes. To study hydrophilic molecules, CHARMM36 is the only FF

able to predict a correct ranking of lipophilicity. However, in the GROMACS software due the specific TIP3P water model required, CHARMM36 is the slowest, which might be limiting for larger systems, such as proteins and lipids. Taking all pros and contras into account, we recommend Slipids as the versatile FF for simulations of complex molecular systems containing lipid bilayers. It should be noted that an inclusion of polarization effects might be successful strategy how to improve predictions of partition coefficients from MD simulations.⁵¹

ASSOCIATED CONTENT

Supporting Information

Table S1: Duration of z-constraint simulations. Table S2: CPU times. Table S3: Calculated and experimental partition coefficients. Table S4: Calculated penetration barriers. Table S5: Calculated water/lipids barriers. Table S6: Calculated positions of free energy minima. Figure S1: Mean difference of free energy profiles with respect to Slipids. This material is available free of charge via the Internet at <http://pubs.acs.org>.

AUTHOR INFORMATION

Corresponding Authors

*Tel: +420 585 634 756. Email: karel.berka@upol.cz.

*Tel: +420 585 634 756. Email: michal.otyepka@upol.cz.

Notes

The authors declare no competing financial interest.

ACKNOWLEDGMENTS

This work was supported by the Grant Agency of the Czech Republic (P208/12/G016), the Operational Program Research and Development for Innovations—European Regional Development Fund (CZ.1.05/2.1.00/03.0058), the Operational Program Education for Competitiveness—European Social Fund (CZ.1.07/2.3.00/20.0058), and a student project of Palacký University (IGA_PrF_2014023). P.T. and G.F. thank the “Conseil Régional du Limousin” for financial support and CALI (CALcul en LIMousin).

REFERENCES

- (1) Alberts, B.; Johnson, A.; Lewis, J.; Raff, M.; Roberts, K.; Walter, P. *Molecular Biology of the Cell*, 4th ed.; Garland Science: New York, 2002.
- (2) Nagle, J. F.; Mathai, J. C.; Zeidel, M. L.; Tristram-Nagle, S. Theory of Passive Permeability through Lipid Bilayers. *J. Gen. Physiol.* **2008**, *131*, 77–85.
- (3) Orsi, M.; Essex, J. W. Passive Permeation Across Lipid Bilayers: A Literature Review. In *Molecular Simulations and Biomembranes*; Sansom, M. S. P., Biggin, P. C., Eds.; Royal Society of Chemistry: Cambridge, U.K., 2010; pp 76–90.
- (4) Ayrton, A.; Morgan, P. Role of Transport Proteins in Drug Absorption, Distribution, and Excretion. *Xenobiotica* **2001**, *31*, 469–497.
- (5) Seddon, A. M.; Casey, D.; Law, R. V.; Gee, A.; Templer, R. H.; Ces, O. Drug Interactions with Lipid Membranes. *Chem. Soc. Rev.* **2009**, *38*, 2509–2519.
- (6) Lúcio, M.; Lima, J. L. F. C.; Reis, S. Drug–Membrane Interactions: Significance for Medicinal Chemistry. *Curr. Med. Chem.* **2010**, *17*, 1795–1809.
- (7) Balaz, S. Modeling Kinetics of Subcellular Disposition of Chemicals. *Chem. Rev.* **2009**, *109*, 1793–1899.
- (8) Cooper, G. M. *The Cell, A Molecular Approach*; Sinauer Associates: Sunderland, MA, 2000.
- (9) Berka, K.; Hendrychová, T.; Anzenbacher, P.; Otyepka, M. Membrane Position of Ibuprofen Agrees with Suggested Access Path

Entrance to Cytochrome P450 2C9 Active Site. *J. Phys. Chem. A* **2011**, *115*, 11248–11255.

(10) Paloncýová, M.; Berka, K.; Otyepka, M. Molecular Insight into Affinities of Drugs and Their Metabolites to Lipid Bilayers. *J. Phys. Chem. B* **2013**, *117*, 2403–2410.

(11) Berka, K.; Paloncýová, M.; Anzenbacher, P.; Otyepka, M. Behavior of Human Cytochromes P450 on Lipid Membranes. *J. Phys. Chem. B* **2013**, *117*, 11556–11564.

(12) Seydel, J. K.; Wiese, M. *Drug-Membrane Interactions: Analysis, Drug Distribution, Modeling*; Mannhold, R., Kubinyi, H., Folkers, G., Eds.; Wiley-VCH Verlag GmbH: Weinheim, 2002; Vol. 4.

(13) Piggot, T. J.; Piñeiro, Á.; Khalid, S. Molecular Dynamics Simulations of Phosphatidylcholine Membranes: A Comparative Force Field Study. *J. Chem. Theory Comput.* **2012**, *8*, 4593–4609.

(14) Košinová, P.; Berka, K.; Wykes, M.; Otyepka, M.; Trouillas, P. Positioning of Antioxidant Quercetin and Its Metabolites in Lipid Bilayer Membranes: Implication for Their Lipid-Peroxidation Inhibition. *J. Phys. Chem. B* **2012**, *116*, 1309–1318.

(15) Podlouncká, P.; Berka, K.; Fabre, G.; Paloncýová, M.; Duroux, J.-L.; Otyepka, M.; Trouillas, P. Lipid Bilayer Membrane Affinity Rationalizes Inhibition of Lipid Peroxidation by a Natural Lignan Antioxidant. *J. Phys. Chem. B* **2013**, *117*, 5043–5049.

(16) Paloncýová, M.; Berka, K.; Otyepka, M. Convergence of Free Energy Profile of Coumarin in Lipid Bilayer. *J. Chem. Theory Comput.* **2012**, *8*, 1200–1211.

(17) Paloncýová, M.; Devane, R.; Murch, B.; Berka, K.; Otyepka, M. Amphiphilic Drug-Like Molecules Accumulate in a Membrane below the Head Group Region. *J. Phys. Chem. B* **2014**, *118*, 1030–1039.

(18) Orsi, M.; Essex, J. W. Permeability of Drugs and Hormones through a Lipid Bilayer: Insights from Dual-Resolution Molecular Dynamics. *Soft Matter* **2010**, *6*, 3797–3808.

(19) Bemporad, D.; Essex, J. W.; Luttmann, C. Permeation of Small Molecules through a Lipid Bilayer: A Computer Simulation Study. *J. Phys. Chem. B* **2004**, *108*, 4875–4884.

(20) Neale, C.; Bennett, W. F. D.; Tieleman, D. P.; Pomès, R. Statistical Convergence of Equilibrium Properties in Simulations of Molecular Solutes Embedded in Lipid Bilayers. *J. Chem. Theory Comput.* **2011**, *7*, 4175–4188.

(21) Jämbeck, J. P. M.; Lyubartsev, A. P. Exploring the Free Energy Landscape of Solutes Embedded in Lipid Bilayers. *J. Phys. Chem. Lett.* **2013**, *4*, 1781–1787.

(22) Marrink, S. J.; Berendsen, H. J. C. Permeation Process of Small Molecules across Lipid Membranes Studied by Molecular Dynamics Simulations. *J. Phys. Chem.* **1996**, *100*, 16729–16738.

(23) Mackerell, A. D. Empirical Force Fields for Biological Macromolecules: Overview and Issues. *J. Comput. Chem.* **2004**, *25*, 1584–1604.

(24) Schlick, T.; Neidle, S.; Scheraga, H. A.; MacKerell, A. D. J. *Innovations in Biomolecular Modeling and Simulations*; Schlick, T., Ed.; RSC Biomolecular Sciences; Royal Society of Chemistry: Cambridge, U.K., 2012; Vol. 1.

(25) Marrink, S. J.; Risselada, H. J.; Yefimov, S.; Tieleman, D. P.; de Vries, A. H. The MARTINI Force Field: Coarse Grained Model for Biomolecular Simulations. *J. Phys. Chem. B* **2007**, *111*, 7812–7824.

(26) Shinoda, W.; DeVane, R.; Klein, M. L. Multi-Property Fitting and Parameterization of a Coarse Grained Model for Aqueous Surfactants. *Mol. Simul.* **2007**, *33*, 27–36.

(27) Berger, O.; Edholm, O.; Jahnig, F. Molecular Dynamics Simulations of a Fluid Bilayer of Dipalmitoylphosphatidylcholine at Full Hydration, Constant Pressure, and Constant Temperature. *Biophys. J.* **1997**, *72*, 2002–2013.

(28) Chiu, S.-W.; Pandit, S. A.; Scott, H. L.; Jakobsson, E. An Improved United Atom Force Field for Simulation of Mixed Lipid Bilayers. *J. Phys. Chem. B* **2009**, *113*, 2748–2763.

(29) Jämbeck, J. P. M.; Lyubartsev, A. P. Derivation and Systematic Validation of a Refined All-Atom Force Field for Phosphatidylcholine Lipids. *J. Phys. Chem. B* **2012**, *116*, 3164–3179.

(30) Jämbeck, J. P. M.; Lyubartsev, A. P. An Extension and Further Validation of an All-Atomistic Force Field for Biological Membranes. *J. Chem. Theory Comput.* **2012**, *8*, 2938–2948.

(31) Jämbeck, J. P. M.; Lyubartsev, A. P. Another Piece of the Membrane Puzzle: Extending Slipids Further. *J. Chem. Theory Comput.* **2012**, *9*, 774–784.

(32) Klauda, J. B.; Venable, R. M.; Freites, J. A.; Connor, J. W. O.; Tobias, D. J.; Mondragon-Ramirez, C.; Vorobyov, I.; Mackerell, A. D.; Pastor, R. W. Update of the CHARMM All-Atom Additive Force Field for Lipids: Validation on Six Lipid Types. *J. Phys. Chem. B* **2010**, *114*, 7830–7843.

(33) Pastor, R. W.; Mackerell, A. D. Development of the CHARMM Force Field for Lipids. *J. Phys. Chem. Lett.* **2011**, *2*, 1526–1532.

(34) Dickson, C. J.; Rosso, L.; Betz, R. M.; Walker, R. C.; Gould, I. R. GAFFlipid: A General Amber Force Field for the Accurate Molecular Dynamics Simulation of Phospholipid. *Soft Matter* **2012**, *8*, 9617–9627.

(35) Skjevik, Å. a.; Madej, B. D.; Walker, R. C.; Teigen, K. LIPID11: A Modular Framework for Lipid Simulations Using Amber. *J. Phys. Chem. B* **2012**, *116*, 11124–11136.

(36) Dickson, C. J.; Madej, B. D.; Skjevik, Å. A.; Betz, R. M.; Teigen, K.; Gould, I. R.; Walker, R. C. Lipid14: The Amber Lipid Force Field. *J. Chem. Theory Comput.* **2014**, *10*, 865–879.

(37) Klamt, A.; Huniar, U.; Spycher, S.; Keldenich, J. COSMOmic: A Mechanistic Approach to the Calculation of Membrane–Water Partition Coefficients and Internal Distributions within Membranes and Micelles. *J. Phys. Chem. B* **2008**, *112*, 12148–12157.

(38) Eckert, F.; Klamt, A. *COSMOtherm*; COSMOlogic GmbH & Co. KG: Leverkusen, Germany, 2013.

(39) Klamt, A. The COSMO and COSMO-RS Solvation Models. *Wiley Interdiscip. Rev. Comput. Mol. Sci.* **2011**, *1*, 699–709.

(40) Endo, S.; Escher, B. I.; Goss, K.-U. Capacities of Membrane Lipids to Accumulate Neutral Organic Chemicals. *Environ. Sci. Technol.* **2011**, *45*, 5912–5921.

(41) Jakobtorweihen, S.; Ingram, T.; Smirnova, I. Combination of COSMOmic and Molecular Dynamics Simulations for the Calculation of Membrane–Water Partition Coefficients. *J. Comput. Chem.* **2013**, *34*, 1332–1340.

(42) Wang, J.; Wolf, R. M.; Caldwell, J. W.; Kollman, P. a.; Case, D. a. Development and Testing of a General Amber Force Field. *J. Comput. Chem.* **2004**, *25*, 1157–1174.

(43) Schüttelkopf, A. W.; van Aalten, D. M. F. PRODRG: A Tool for High-Throughput Crystallography of Protein-Ligand Complexes. *Acta Crystallogr. Sect. D Biol. Crystallogr.* **2004**, *60*, 1355–1363.

(44) Vanommeslaeghe, K.; Mackerell, A. D. Automation of the CHARMM General Force Field (CGenFF) I: Bond Perception and Atom Typing. *J. Chem. Inf. Model.* **2012**, *52*, 3144–3154.

(45) Vanommeslaeghe, K.; Raman, E. P.; Mackerell, A. D. Automation of the CHARMM General Force Field (CGenFF) II: Assignment of Bonded Parameters and Partial Atomic Charges. *J. Chem. Inf. Model.* **2012**, *52*, 3155–3168.

(46) Dupradeau, F.-Y.; Pigache, A.; Zaffran, T.; Savineau, C.; Lelong, R.; Grivel, N.; Lelong, D.; Rosanski, W.; Cieplak, P. The R.E.D. Tools: Advances in RESP and ESP Charge Derivation and Force Field Library Building. *Phys. Chem. Chem. Phys.* **2010**, *12*, 7821–7839.

(47) Woods, R. J.; Khalil, M.; Pell, W.; Moffat, S. H.; Smith, V. H. Net Atomic Charges from Molecular Electrostatic Potentials. *J. Comput. Chem.* **1990**, *11*, 297–310.

(48) Frisch, M. J.; Trucks, G. W.; Schlegel, H. B.; Scuseria, G. E.; Robb, M. A.; Cheeseman, J. R.; Scalmani, G.; Barone, V.; Mennucci, B.; Petersson, G. A.; et al. *Gaussian 09*, Revision A.02, Gaussian, Inc.: Wallingford, CT, 2009.

(49) Cieplak, P.; Caldwell, J.; Kollman, P. Molecular Mechanical Models for Organic and Biological Systems Going Beyond the Atom Centered Two Body Additive Approximation: Aqueous Solution Free Energies of Methanol and N-Methyl Acetamide, Nucleic Acid Base, and Amide Hydrogen Bonding and Chloroform/Water Partition Coefficients of the Nucleic Acid Bases. *J. Comput. Chem.* **2001**, *22*, 1048–1057.

- (50) Cornell, W. D. A Second Generation Force Field for the Simulation of Proteins, Nucleic Acids, and Organic Molecules. *J. Am. Chem. Soc.* **1995**, *117*, 5179–5197.
- (51) Jämbeck, J. P. M.; Lyubartsev, A. P. Implicit Inclusion of Atomic Polarization in Modeling of Partitioning Between Water and Lipid Bilayers. *Phys. Chem. Chem. Phys.* **2013**, *15*, 4677–4686.
- (52) Katz, Y.; Diamond, J. M. Thermodynamic Constants for Nonelectrolyte Partition between Dimyristoyl Lecithin and Water. *J. Membr. Biol.* **1974**, *17*, 101–120.
- (53) Vaes, W. H.; Ramos, E. U.; Hamwijk, C.; van Holsteijn, I.; Blaauboer, B. J.; Seinen, W.; Verhaar, H. J.; Hermens, J. L. Solid Phase Microextraction as a Tool to Determine Membrane/Water Partition Coefficients and Bioavailable Concentrations in In Vitro Systems. *Chem. Res. Toxicol.* **1997**, *10*, 1067–1072.
- (54) Gobas, F. A. P. C.; Lahittete, J. M.; Garofalo, G.; Shiu, W. Y.; Mackay, D. A Novel Method for Measuring Membrane–Water Partition Coefficients of Hydrophobic Organic Chemicals: Comparison with 1-Octanol–Water Partitioning. *J. Pharm. Sci.* **1988**, *77*, 265–272.
- (55) Van der Heijden, S. A.; Jonker, M. T. O. Evaluation of Liposome–Water Partitioning for Predicting Bioaccumulation Potential of Hydrophobic Organic Chemicals. *Environ. Sci. Technol.* **2009**, *43*, 8854–8859.
- (56) Nagle, J. F.; Tristram-Nagle, S. Structure of Lipid Bilayers. *Biochim. Biophys. Acta* **2000**, *1469*, 159–195.
- (57) Darden, T.; York, D.; Pedersen, L. Particle Mesh Ewald: An $N \log(N)$ Method for Ewald Sums in Large Systems. *J. Chem. Phys.* **1993**, *98*, 10089–10092.
- (58) Hess, B.; Bekker, H.; Berendsen, H. J. C.; Fraaije, J. G. E. M. LINCS: A Linear Constraint Solver for Molecular Simulations. *J. Comput. Chem.* **1997**, *18*, 1463–1472.
- (59) Parrinello, M.; Rahman, A. Polymorphic Transitions in Single Crystals: A New Molecular Dynamics Method. *J. Appl. Phys.* **1981**, *52*, 7182–7190.
- (60) Nosé, S. A Unified Formulation of the Constant Temperature Molecular Dynamics Methods. *J. Chem. Phys.* **1984**, *81*, 511.
- (61) Hoover, W. G. Canonical Dynamics: Equilibrium Phase-Space Distributions. *Phys. Rev. A* **1985**, *31*, 1695–1697.
- (62) Berendsen, H. J. C.; Postma, J. P. M.; Gunsteren, W. F. van; Hermans, J. Interaction Models for Water in Relation to Protein Hydration. In *Intermolecular Forces*; Pullman, B., Ed.; Reidel Publishing Company, 1981; pp 331–338.
- (63) Berendsen, H. J. C.; Grigera, J. R.; Straatsma, T. P. The Missing Term in Effective Pair Potentials. *J. Phys. Chem.* **1987**, *91*, 6269–6271.
- (64) Durell, S. R.; Brooks, B. R.; Ben-Naim, A. Solvent-Induced Forces between Two Hydrophilic Groups. *J. Phys. Chem.* **1994**, *98*, 2198–2202.
- (65) Jorgensen, W. L.; Chandrasekhar, J.; Madura, J. D.; Impey, R. W.; Klein, M. L. Comparison of Simple Potential Functions for Simulating Liquid Water. *J. Chem. Phys.* **1983**, *79*, 926.
- (66) MacCallum, J. L.; Bennett, W. F. D.; Tieleman, D. P. Distribution of Amino Acids in a Lipid Bilayer from Computer Simulations. *Biophys. J.* **2008**, *94*, 3393–3404.
- (67) Becke, A. D. Density-Functional Exchange-Energy Approximation with Correct Asymptotic Behavior. *Phys. Rev. A* **1988**, *38*, 3098–3100.
- (68) Perdew, J. P. Density-Functional Approximation for the Correlation Energy of the Inhomogeneous Electron Gas. *Phys. Rev. B* **1986**, *34*, 7406.
- (69) Klamt, A. *COSMO-RS: From Quantum Chemistry to Fluid Phase Thermodynamics and Drug Design*; Elsevier Science Ltd.: Amsterdam, 2005.
- (70) Meloun, M.; Bordovská, S.; Kupka, K. Outliers Detection in the Statistical Accuracy Test of a pK_a Prediction. *J. Math. Chem.* **2010**, *47*, 891–909.
- (71) Leftin, A.; Brown, M. F. An NMR Database for Simulations of Membrane Dynamics. *Biochim. Biophys. Acta* **2011**, *1808*, 818–839.